School Closure and Mitigation of Pandemic (H1N1) 2009, Hong Kong

Joseph T. Wu, Benjamin J. Cowling, Eric H.Y. Lau, Dennis K.M. Ip, Lai-Ming Ho, Thomas Tsang, Shuk-Kwan Chuang, Pak-Yin Leung, Su-Vui Lo, Shao-Haei Liu, and Steven Riley

In Hong Kong, kindergartens and primary schools were closed when local transmission of pandemic (H1N1) 2009 was identified. Secondary schools closed for summer vacation shortly afterwards. By fitting a model of reporting and transmission to case data, we estimated that transmission was reduced ≈25% when secondary schools closed.

The emergence and subsequent global spread of pandemic (H1N1) 2009 presents several challenges to health policy makers. Although some countries have substantial antiviral drug stockpiles available for treatment and chemoprophylaxis and vaccines became available toward the end of 2009, nonpharmaceutical interventions remain the primary resource available to most populations to mitigate the impact of pandemic (H1N1) 2009 (*1*). One such nonpharmaceutical intervention is school closure, either reactively following outbreaks or proactively at district or regional levels (*2*,*3*). A recent review has highlighted the lack of consensus over the potential benefits of school closures and the potential economic and social costs (*4*). Although the current pandemic (H1N1) 2009 virus is of moderate severity, data from 2009 provide an ideal opportunity to estimate the effectiveness of interventions against pandemic influenza.

In Hong Kong Special Administrative Region, People's Republic of China, there was a considerable delay between the first reported imported case on May 1, 2009, and the first reported local case (i.e., not otherwise epidemiologically linked with outside travel, contact with an imported case-patient, or contact with an infected person who had contact with an imported case-patient) was laboratory-confirmed and reported to the government on June 10. During the initial stages of the epidemic, the local government operated under containment phase protocols, in which all confirmed cases were isolated in hospital and their contacts were traced, quarantined in hotels, hospitals, and holiday camps, and provided with antiviral drug prophylaxis. When the first nonimported case was confirmed, the government entered the mitigation phase and announced immediate closure of all primary schools, kindergartens, childcare centers and special schools, initially for 14 days. Closures were subsequently continued until the summer vacation began July 10. Secondary schools generally remained open, while those with ≥1 confirmed case were immediately closed for 14 days. Some containment-phase policies, including isolation of cases and prophylaxis of contacts, were maintained until June 27. During our study period, patients seeking treatment for suspected influenza at designated fever clinics and public hospital emergency departments were routinely tested, and pandemic (H1N1) 2009 virus infection was a reportable infectious disease.

Author affiliations: The University of Hong Kong School of Public Health, Hong Kong Special Administrative Region, People's Republic of China (J.T. Wu, B.J. Cowling, E.H.Y. Lau, D.K.M. Ip, L.-M. Ho, S. Riley); Centre for Health Protection, Hong Kong (T. Tsang, S.-K. Chuang); Hospital Authority, Hong Kong (P.-Y. Leung, S.-V. Lo, S.-H Liu); and Food and Health Bureau, Hong Kong (S.-V. Lo)

DOI: 10.3201/eid1603.091216

The Study

We analyzed epidemiologic data on laboratory-confirmed pandemic (H1N1) 2009 infections collected by the Hong Kong Hospital Authority and Centre for Health Protection (the e-flu database). The epidemic curve of laboratory-confirmed pandemic (H1N1) 2009 cases showed a biphasic pattern, with a small initial peak in reported cases at the end of June followed by a nadir at the beginning of July and rising incidence after that (Figure, panel A).

We specified an age-structured susceptible-infectious-recovered transmission model to explain the early pandemic (H1N1) 2009 dynamics in Hong Kong (online Technical Appendix, www.cdc.gov/EID/content/16/3/538-Techapp.pdf). We estimated change points in the proportion of symptomatic infections identified and age-specific rates of seeding of infectious cases from overseas. A simple 3-period model for changes in reporting rates provided a parsimonious fit to the data (Figure, panel B). Reporting rates were defined relative to the initial reporting rate. The comparison between the observed and estimated incidence is shown in the Figure, panel C.

We estimated that the relative rate of reporting declined to ≈5.2% of its initial value from June 29 onward (Table). Persons <19 years of age were estimated to be 2.6× more susceptible than the rest of the population. The estimated effective reproductive number was 1.7 before educational institutions for children <13 years of age were closed on June 11, 1.5 between June 11 and July 10 when summer vacation began, and 1.1 for the rest of the summer. The drop in reproductive number was driven by an estimated 70% reduction in intra–age-group transmission concurrent with school closures. The fitted model implies that ≈182,000 persons (2.5%

of the population) had experienced illness associated with pandemic (H1N1) 2009 infection by August 27.

Figure, panel D shows that in the period from the first confirmed local case to the start of summer vacation on July 10, there were a substantial number of cases among older children (whose schools remained open) but few among younger children (whose schools were closed during this period). Only 10% of Hong Kong residents are young children ≤12 years of age, 8% are older children 13–18 years of age, and 82% are adults.

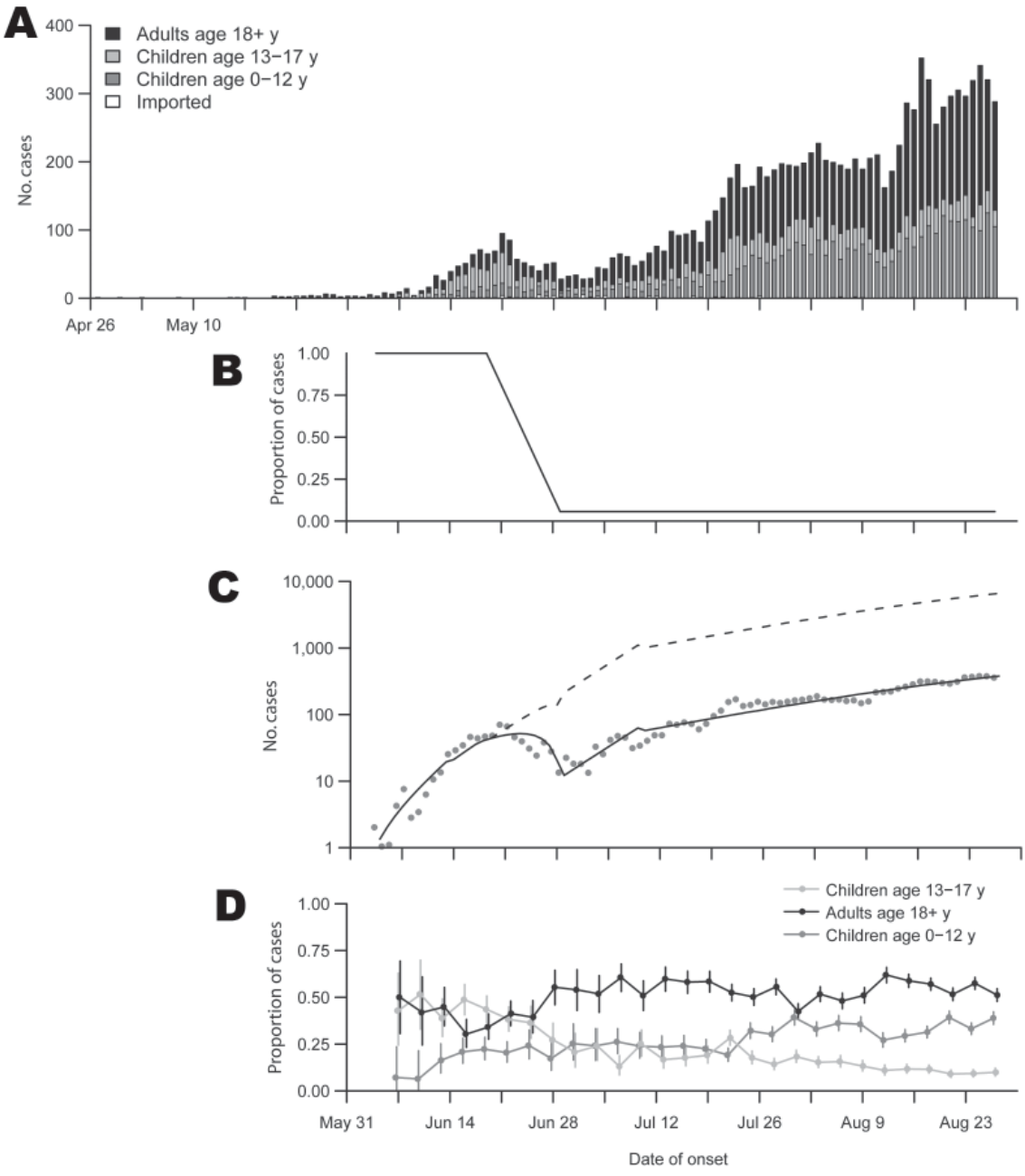

Figure. Epidemiologic characteristics of pandemic (H1N1) 2009 in Hong Kong Special Administrative Region, People's Republic of China, during May through August 2009. A) Time series of laboratory-confirmed pandemic (H1N1) 2009 cases classified as imported or nonimported (by age group) by date of illness onset. B) Estimates of the proportion of cases with illness onset on each day that would subsequently be identified and laboratory confirmed (reporting rates). C) Time series of nonimported pandemic (H1N1) 2009 cases by date of illness onset and the estimates of the underlying true epidemic curve (dashed line) and the fitted observed epidemic curve allowing for changes in reporting rates (solid line). Dots indicate cases reported on a given day. Number of cases plotted logarithmically. D) Distribution of ages of laboratory-confirmed pandemic (H1N1) 2009 cases over time plotted as 3-day rolling averages. Error bars indicate 95% confidence intervals.

Table. Summary statistics of posterior distributions obtained by using Markov Chain Monte Carlo in modeling the effects of school closures on mitigating a pandemic (H1N1) 2009 outbreak, Hong Kong, 2009*

Parameter†	Posterior mean (SD)	95% CI
M_i, daily number of effective seeds in age class i, I = 1,2,3	<13 y: 0.1 (0.1)	0–0.04
	13–19 y: 0.4 (0.1)	0.2–0.6
	>19 y: 0.2 (0.2)	0–0.6
Basic reproductive number	Before Jun 11: 1.71 (0.04)	1.63–1.78
Relative susceptibility of persons <20 y of age	2.64 (0.08)	2.48–2.78
Percentage reduction in intra-age-group transmission given by school closures	70% (3%)	64%–75%
t_1, the date at which reporting rates began to decline	Jun 18 (1.2 d)	Jun 17–Jun 21
t_2, the date at which reporting rates stopped declining	Jun 29 (0.3 d)	Jun 29–Jun 30
r_2, the reporting rate after t_2	5.2% (1.1%)	3.5%–7.7%

*CI, confidence interval.
†Model assumes a linear decline in reporting rates from 100% to r_2 between times t_1 and t_2.

Conclusions

In Hong Kong, kindergartens and primary schools were closed when local transmission of pandemic influenza was identified. By using a parsimonious transmission model to interpret age-specific reporting data, we concluded that the subsequent closure of secondary schools for the summer vacation was associated with substantially lower transmission across age groups. We estimated that reporting of cases declined to 5.2% of its initial rate through the second half of June; this is plausible given the gradual change from containment phase to mitigation phase over that period.

It is challenging to infer the precise impact of school closures in Hong Kong, given that they were implemented immediately and sustained until summer vacation and so we have little data on local transmissibility in the absence of school closures. In previous pandemics attack rates have generally been highest in younger children (*4*,*5*), and this has been noted for pandemic (H1N1) 2009 in Mexico (*6*) and Chicago (*7*). This observation, in combination with our finding that children <12 years of age were relatively unaffected in Hong Kong during the school closure period (Figure, panel D), intuitively implies that closures were effective in preventing infections in this age group. Furthermore, assuming that children are responsible for up to half of all community transmission (*8*), it is likely that protection of younger children had substantial indirect benefits. Previous studies have suggested that sustained school closures during a pandemic could reduce peak attack rates and prevent 13%–17% of total cases in France (*8*) or ≤20% of total cases in the United Kingdom (*3*). Our finding that the reproductive number declined from 1.5 during the kindergarten and primary school closures to 1.1 during summer vacation suggests that a much more substantial drop in attack rates would result from sustained school closures.

By including a model of reporting, we have also been able to estimate case numbers. We estimated a cumulative illness attack rate of ≈182,000 cases (2.5% of the population) by August 27. Between June 29 and August 27, a total of 1,522/9,846 confirmed pandemic (H1N1) 2009 case-patients were hospitalized for medical reasons, among whom 13 died. These numbers are more consistent with a substantially lower case-fatality ratio than suggested by initial estimates of the severity of the pandemic (H1N1) 2009 strain (*9*,*10*). These estimates are dependent on the initial rate of reporting being close to 100%.

We assumed that transmission varied by age and time. If reporting rates varied in a way not accounted for by our model, this would affect the accuracy of our estimates of growth rate and cumulative attack rates. Although we attributed changes in transmissibility between June and August to school closures and summer vacations, it is possible that other secular changes or external factors such as seasonality also contributed. However, it is unlikely that seasonal factors would have reduced transmission of influenza at this time of year, on the basis of symptomatic and laboratory confirmed incidence of influenza from previous years (*11*). Reference data on age-specific population attack rates from serologic surveys or population-based surveillance systems would enable us to calibrate our estimates of reporting rates and growth rates and provide external validation of our model estimates.

Acknowledgments

We acknowledge the Hospital Authority Strategy and Planning Division, Hospital Authority Information Technology Division, and the Centre for Health Protection for the collation of the e-flu database. We thank Max Lau for assistance in drawing the Figure. We thank Kwok Kin On and Danny Yao for helpful discussions.

This research received financial support from the Research Fund for the Control of Infectious Disease, Food and Health Bureau, Government of the Hong Kong Special Administrative Region (grant no. HK-09-04-01); the Harvard Center for Communicable Disease Dynamics from the US National Institutes of Health Models of Infectious Disease Agent Study program (grant no. 1 U54 GM088558); the Area of Excellence Scheme of the Hong Kong University Grants Committee (grant no. AoE/M-12/06); from Fogarty International Center (grant no. 3R01TW008246-01S1); and the Research and Policy for Infectious Disease Dynam-

ics program from Fogarty International Center and the Science & Technology Directorate, Department of Homeland Security.

Dr Wu is assistant professor at the University of Hong Kong School of Public Health. His research interests include using mathematical models to devise effective strategies for the control and mitigation of infectious diseases.

References

1. Bell DM; World Health Organization Writing Group. Nonpharmaceutical interventions for pandemic influenza, national and community measures. Emerg Infect Dis. 2006;12:88–94.
2. Markel H, Lipman HB, Navarro JA, Sloan A, Michalsen JR, Stern AM, et al. Nonpharmaceutical interventions implemented by US cities during the 1918–1919 influenza pandemic. JAMA. 2007;298:644–54. DOI: 10.1001/jama.298.6.644
3. Vynnycky E, Edmunds WJ. Analyses of the 1957 (Asian) influenza pandemic in the United Kingdom and the impact of school closures. Epidemiol Infect. 2008;136:166–79.
4. Cauchemez S, Ferguson NM, Wachtel C, Tegnell A, Saour G, Duncan B, et al. Closure of schools during an influenza pandemic. Lancet Infect Dis. 2009;9:473–81. DOI: 10.1016/S1473-3099(09)70176-8
5. Glezen WP. Emerging infections: pandemic influenza. Epidemiol Rev. 1996;18:64–76.
6. Chowell G, Bertozzi SM, Colchero MA, Lopez-Gatell H, Alpuche-Aranda C, Hernandez M, et al. Severe respiratory disease concurrent with the circulation of H1N1 influenza. N Engl J Med. 2009;13;361:674-9.
7. Centers for Disease Control and Prevention. 2009 pandemic influenza A (H1N1) virus infections—Chicago, Illinois, April–July 2009. MMWR Morb Mortal Wkly Rep. 2009;58:913–8.
8. Cauchemez S, Valleron AJ, Boelle PY, Flahault A, Ferguson NM. Estimating the impact of school closure on influenza transmission from sentinel data. Nature. 2008;452:750–4. DOI: 10.1038/nature06732
9. Fraser C, Donnelly CA, Cauchemez S, Hanage WP, Van Kerkhove MD, Hollingsworth TD, et al. Pandemic potential of a strain of influenza A (H1N1): early findings. Science. 2009;324:1557–61. DOI: 10.1126/science.1176062
10. Wilson N, Baker MG. The emerging influenza pandemic: estimating the case fatality ratio. Euro Surveill. 2009;14:1–4.
11. Cowling BJ, Wong IO, Ho LM, Riley S, Leung GM. Methods for monitoring influenza surveillance data. Int J Epidemiol. 2006;35:1314–21. DOI: 10.1093/ije/dyl162

Address for correspondence: Benjamin J. Cowling, School of Public Health, The University of Hong Kong, Units 624-7, Cyberport 3, Pokfulam, Hong Kong Special Administrative Region, People's Republic of China; email: bcowling@hku.hk

www.cdc.gov/eid

EMERGING INFECTIOUS DISEASES®

To subscribe online:
http://www.cdc.gov/ncidod/EID/subscrib.htm

☐ Subscribe to print version
☐ Unsubscribe from print version
☐ Update mailing address

Number on mailing label:_____

Name:

_____

Full mailing address: (BLOCK LETTERS)

Return:

Email:
eideditor@cdc.gov

Fax: 404-639-1954

or mail to:

EID Editor
CDC/NCID/MS D61
1600 Clifton Rd, NE
Atlanta, GA 30333
USA

School Closure and Mitigation of Pandemic (H1N1) 2009, Hong Kong

Technical Appendix

Technical Details of the Transmission Model and Sensitivity Analyses

Transmission Model

We specified an age-structured Susceptible-Infectious-Recovered model with 3 age classes (<13 years old, 13–19 years old, and >19 years old) to describe the transmission dynamics of influenza A pandemic (H1N1) 2009 in Hong Kong Special Administrative Region, People's Republic of China. The local epidemic was seeded by sporadic imported cases since April 2009. We modeled the seeding force of infection by assuming an effective seed size of M_i per day for class i starting 3 days before the first known symptom onset date of a nonimported case on June 4. The who-acquired-infection-from-whom (WAIFW) matrix W was constructed as follows. First, using recently published social contact data (*1*), we constructed a contact matrix $C = \{C_{ij}\}$ where C_{ij} was the average number of class i contacts that class j individual had per day. The WAIFW matrix W was then constructed from C by 1) assuming that age classes 1 and 2 were h times more susceptible than class 3 (*2*), and 2) scaling the resulting matrix such that the largest eigenvalue of the corresponding next generation matrix was equal to R_0.

We made the following assumptions regarding temporal changes in transmissibility of the virus. Transmissibility remained constant before June 11, the date on which the government announced immediate closure of all primary schools, kindergartens, child-care centers and special schools. Starting on June 11, transmissibility within age class 1 was reduced by a proportion q because of this intervention (i.e., W_{11} was discounted by a factor $1 - q$). Similarly, beginning on July 10 (the start of summer holidays for secondary schools), transmissibility within age class 2 was reduced by the same proportion q. Transmissibility of the virus then remained constant throughout the summer. In summary, the epidemic was simulated by using the following differential equations. For $i = 1, 2, 3$,

$$\frac{dS_i(t)}{dt} = -S_i(t)\sum_{j=1}^{3} W_{ij}(t)\frac{I_j(t)}{N_i},$$
$$\frac{dI_i(t)}{dt} = -\frac{dS_i(t)}{dt} - \frac{I_i(t)}{D_I} + M_i,$$

where N_i was the size of age class i, $S_i(t)$ and $I_i(t)$ were the number of susceptible and infectious class i persons at time t, $\{W_{ij}(t)\}$ was the WAIFW matrix (time-dependent as described above), and D_I was the mean infectious duration. We assumed $D_I = 3$ days, but our results were insensitive to this assumption (see Sensitivity Analyses below). The parameters R_0, M_i, h and q were estimated by using Markov Chain Monte Carlo (MCMC) methods under a Bayesian inferential framework.

Reporting Rate

We assumed that the proportion of case-patients who reported symptoms to the health officials was described by the following function:

$$r(t) = \begin{cases} 1 & \text{if } t < t_1, \\ 1 + \dfrac{r_2 - 1}{t_2 - t_1}(t - t_1) & \text{if } t_1 \le t \le t_2, \\ r_2 & \text{if } t > t_2, \end{cases}$$

where $0 < r_2 < 1$. That is, we assumed 100% reporting rate before time t_1. The parameters t_1, t_2, and r_2 were estimated by using MCMC (see below).

Statistical Inference

We estimated model parameters based on the time series data of the daily number of confirmed nonimported cases with symptom onset from June 4 through August 27. To this end, we first constructed a likelihood function from the transmission model and the reporting rate model:

$$L(M_1, M_2, M_3, R_0, h, q, t_1, t_2, r_2) = \left(\prod_{i=1}^{3} \prod_{t=1}^{t_A} \frac{(\lambda_{it})^{n_{it}} e^{-\lambda_{it}}}{n_{it}!} \right) \prod_{t=t_A+1}^{t_{\max}} \frac{(\lambda_t)^{n_t} e^{-\lambda_t}}{n_t!}$$

where t_A was the number of days for which age-specific onset data were available (from Jun 4 to Aug 10), λ_{it} and n_{it} were the expected and observed number of onsets in age class i on day t, λ_t and n_t were the expected and observed total number of onsets on day t.

The dataset included 9,918 confirmed cases. The date of symptom onset was available for 4,777 cases. To handle the missing data, we first obtained the empirical cumulative density function (cdf) F_i for the age-specific time delay (x_i) between symptom onset and case confirmation for these 4,777 cases. Technical Appendix Figure 1 displays the resulting histograms. We then assumed that the delay between symptom onset and confirmation for the remaining 5,141 cases followed the same empirical distributions. Following the EM algorithm, we took expectation of the n_{it}'s and n_t's in the likelihood function with respect to these cdfs for cases whose dates of symptoms onset were missing.

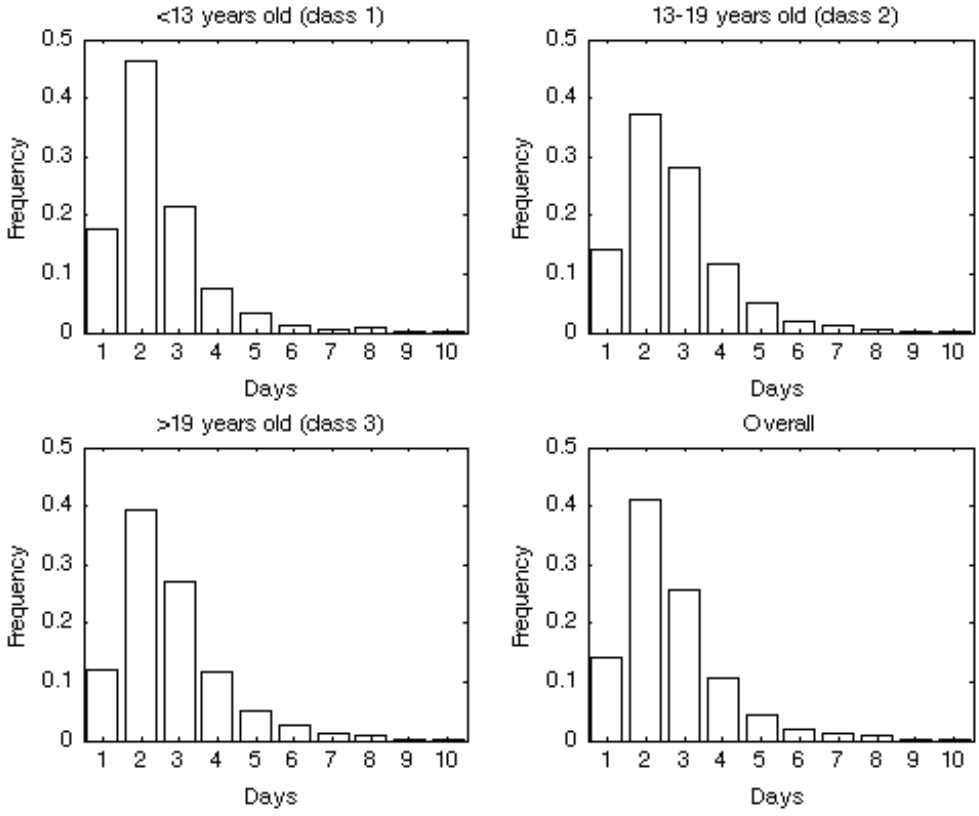

Technical Appendix Figure 1. Histograms for the age-specific and overall time delay between symptoms onset and case confirmation.

Markov Chain Monte Carlo

To simplify the statistical inference procedure and parameter interpretation, we reparameterized the model as follows:

$$t_2 = \alpha_2 t_{\max},$$

$$t_1 = \alpha_1 t_2 = \alpha_1 \alpha_2 t_{\max}.$$

After reparameterization, we assumed flat (i.e., uninformative) prior distributions for all parameters. The prior distributions are given in the Technical Appendix Table.

Technical Appendix Table. Prior distributions and parameter bounds for calculation of posterior distributions using Markov Chain Monte Carlo.

Parameter	Prior	Lower-bound	Upper-bound
M_i, i = 1,2,3	Uniform	0	10
R_0	Uniform	1	2
q	Uniform	0	1
α_1	Uniform	0	1
α_2	Uniform	0	1
r_2	Uniform	0	1
h	Uniform	0	5

To obtain the posterior distributions, we used a random walk metropolis algorithm in which a random step size is chosen for each parameter at every iteration. The step size for a parameter was a uniform random variable with maximum size equal to 1/500 of the feasible range of the parameter (i.e., [upperbound – lowerbound]/500). The MCMC was run for 3,000,000 iterations and the posterior distributions were obtained by using the final 2,000,000 iterations. The acceptance proportion was ≈36%. The results are shown in the Table in the main text and in Appendix Figure 2 below. The posteriors were all distinct from their priors. Chains with different starting points gave similar posterior distributions.

Sensitivity Analyses

We checked the robustness of our results by varying the mean infectious durations D_I from 2 to 4 days. The results were similar to those in the Technical Appendix Table and Technical Appendix Figure 2.

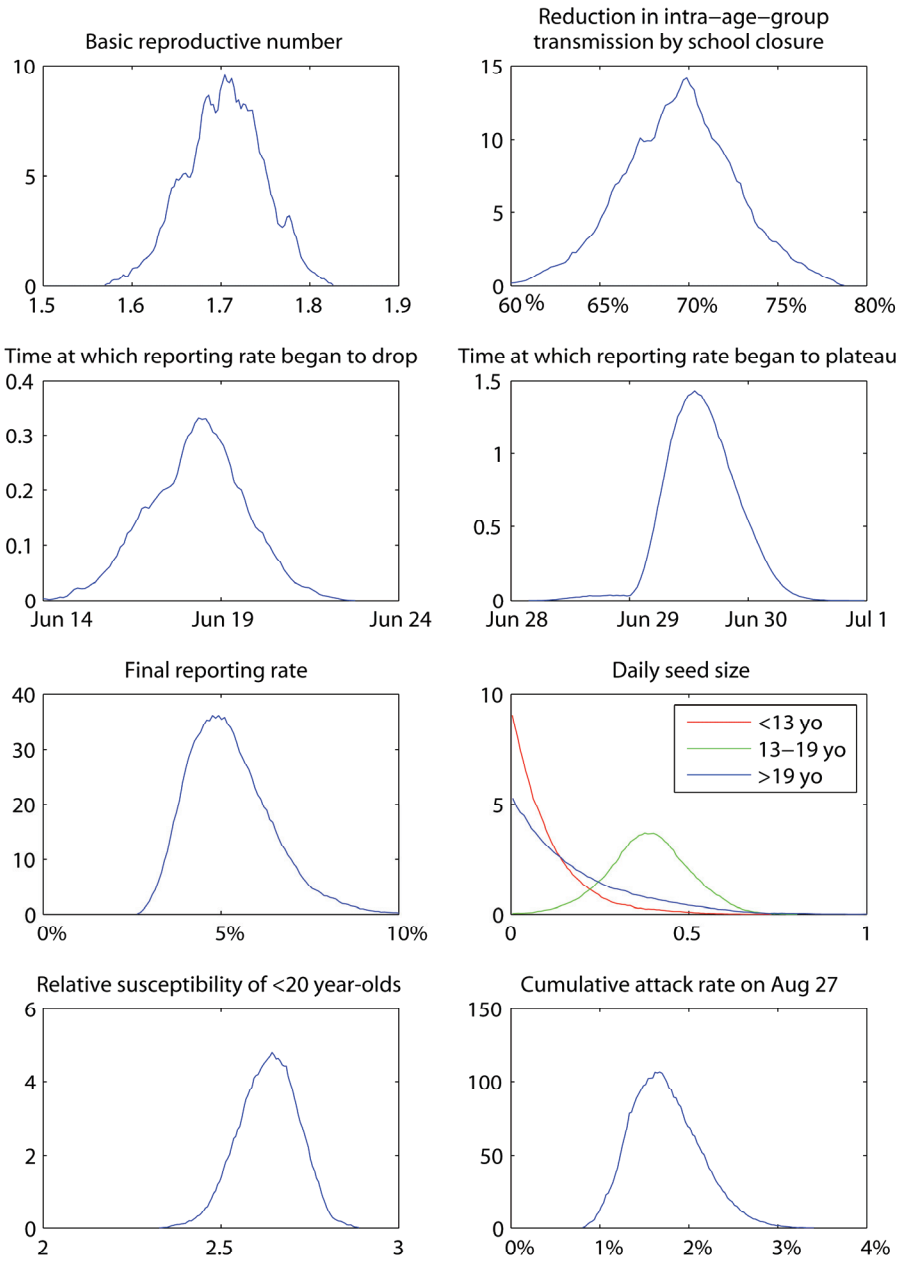

Technical Appendix Figure 2. Posterior distributions of parameters.

References

1. Mossong J, Hens N, Jit M, Beutels P, Auranen K, Mikolajczyk R, et al. Social contacts and mixing patterns relevant to the spread of infectious diseases. PLoS Med. 2008;5:e74. PubMed DOI: 10.1371/journal.pmed.0050074

2. Fraser C, Donnelly CA, Cauchemez S, Hanage WP, Van Kerkhove MD, Hollingsworth TD, et al. Pandemic potential of a strain of influenza A (H1N1): early findings. Science. 2009;324:1557–61. PubMed DOI: 10.1126/science.1176062